vibration

MDPI

Article

Field Experiments and Numerical Analysis of the Ground Vibration Isolation of Shock Wave Propagation under Explosion Shock Loading

Iau-Teh Wang

Department of Civil Engineering, R.O.C. Military Academy, Kaohsiung 83059, Taiwan; itwangroc@gmail.com

Received: 27 August 2019; Accepted: 1 November 2019; Published: 3 November 2019

Abstract: Because blast effects can jeopardize the safety of facilities, controlling blast hazards is critical in engineering design and construction. The attenuation and amplification effects generated by blast waves are affected by the topography and terrain of the blast area. This study examined the effects of topography on the propagation of seismic waves induced by explosions. From the perspective of explosion control, this study adopted explosion mechanics theories and conducted in situ explosion tests to verify finite element numerical simulation results. This study employed the finite element analysis program, to construct a 3D solid structural model to examine fluid–solid coupling, and the Multi-Material Arbitrary Lagrangian–Eulerian algorithm was adopted to develop a dynamic numerical analysis model. By analyzing the propagation of blast waves and ground vibration effects, this study examined the impact of topographical differences on blast effects. The study results may provide a reference for controlling vibration hazards subject to shock waves from explosions, in order to reduce vibrations.

Keywords: blast; explosion; terrain; ground vibration; shock wave; seismic wave

1. Introduction

The energy released by an explosion generates dynamic pressure. Shock waves generated from explosions can damage buildings and facilities, thus affecting residential safety. Because blast effects can jeopardize the safety of facilities, controlling blast hazards has become critical in engineering design and execution. Methods of controlling explosion sources and blocking the propagation path of blast waves are generally adopted to control blast hazards, minimize the effects of denotation energy, and achieve safety protection and prevention goals [1]. Analyzing topographical effects on a site, by using such environmental factors as the geologic materials, space and the dynamic characteristics of seismic waves has become a crucial topic in research on explosion protection engineering.

Blast analysis mainly adopts in situ testing and numerical simulation analysis as research methodologies. Wang [2] and Wang et al. [3] have analyzed the effects of explosions, verified numerical analysis results using experimental data, and confirmed that the LS-DYNA finite element (FE) program is effective for analyzing the propagation characteristics of blast waves generated from ground surface explosions. Goodman [4] confirmed that differences in blast pressure are larger proximal to explosion sources, and so the optimal condition for obtaining data for blast analysis is when the distance between the explosion and the observation point is more than eight times the radius of the explosion. The work of Kivity et al. [5] revealed that the peak free field overpressure was approximately 33% of the ground surface overpressure that would have been generated by the same charge as a semispherical bare explosive; through experimental and numerical analyses, they indicated that the relative error of the blast pressure was 15%. Koga and Matsuo [6] observed that the energy from ground explosions is partially transformed into seismic waves, inducing particle vibrations in the medium. Wang and Lu [7]

indicated that shock waves proximal to an explosion are high in velocity and intensity, corresponding to relatively higher energies from soil compression waves, and thus can serve as a critical parameter for examining ground vibrations. The hazard levels of blast waves can be analyzed by examining the seismic intensity of ground explosions. When analyzing the propagation process of blast waves and the consequences of vibrations, previous studies have used peak particle velocity (PPV), peak particle acceleration (PPA), and peak ground acceleration (PGA) as physical quantities, to assess the seismic intensity of explosions [8–10].

The topography of a site attenuates and amplifies the effects of blast waves. The work of Ahmad et al. [11] adopted a boundary element method, to examine the effectiveness of open and in-filled trenches in screening surface wave propagation, and revealed that the parameters affecting the efficiency of wave screening included the frequency, extent of affected area, trench location, wave velocity, in-fill material properties, Poisson's ratio of the soil and the damping ratio. When the depth of open trenches optimizes the screening effectiveness, the effect of the trench width is negligible, whereas both depth and width are equally critical for in-filled trenches. The work of Klein et al. [12] employed a 3D direct boundary element method to examine the vibration isolation effectiveness of open trenches; typical screening problems when using onsite measurement results were identified, and trench depth was found to be the primary factor affecting screening efficiency. Spyros and Fotis [13] employed the FE method to analyze the propagation of blast waves in obstructed terrain and observed higher particle vibrations in convex terrain than in concave terrain. Nevertheless, the simulation results of such numerical analysis models must be verified using experimental data. Dally and David [14] conducted a series of photoelastic tests to analyze the propagation of Rayleigh waves through convex steps and found that the intensity of particle vibrations increased with step height and wave length. Similarly, Zhu and Yang [15] conducted photoelastic tests to show that the attenuation of blast waves is affected more by the depth of concave terrain than by the width. Through in situ testing, Zhang et al. [16] observed that the attenuation coefficient of the peak velocity was 4.7–87.0% when blast waves propagate through concave landforms, and that the attenuation degree is associated with the scale of concave terrain. To reduce vibration intensity, topographical characteristics can be used to clarify the impact of terrain elevation on the propagation of blast waves, thereby controlling the vibration intensity and preventing potential disasters. Therefore, this study employed in situ explosion testing and a numerical analysis method, to examine the impact of topography on ground explosions, the findings of which may serve as a reference for vibration reduction, disaster prevention and explosion disaster control.

2. Field Experiments and Numerical Analysis

Controlling explosion hazards requires effectively screening the propagation of blast wave energy. From the perspective of vibration control, this study analyzed how the geometrical features of convex and concave terrains affect the propagation of blast wave energy. By implementing in situ explosion testing and a numerical analysis method, this study examined the attenuation and amplification characteristics of blast wave energy and explored the vibration isolation effects generated from various terrain types.

2.1. Explosion Tests

The purpose of the explosion tests was to measure the physical quantity of ground acceleration. To prevent potential risks during the explosion tests, the tests were mainly conducted in concave terrain, where vibration isolation effects were measured, to verify the accuracy of the numerical analysis. The experimental instruments were accelerometers, oscilloscopes, signal conditioners, a power supply system and a data acquisition system. The accelerometers were used to measure the ground acceleration during the explosion tests. The data acquisition system was employed to transfer and save data through the connected oscilloscope and signal conditioner.

Figure 1 displays the setup for concave terrain explosion tests. In the tests, a fixed amount of 226.796 g (0.5 lb) of trinitrotoluene (TNT) was placed vertically and in contact with the ground surface. The distance from the center of explosive charge to the concave terrain was 200 cm. The concave terrain types were all 100 cm in length (width × depth: Case 1 = 50 cm × 30 cm; Case 2 = 70 cm × 30 cm; Case 3 = 90 cm × 30 cm; Case 4 = 30 cm × 60 cm). The vertical axial accelerometers (model number 352C16; sensitivity 1.032 mV/m/s^2) were set at the front and rear of each concave terrain case, to measure the vertical ground acceleration and analyze the effects of the terrain width and depth on the propagation of blast waves.

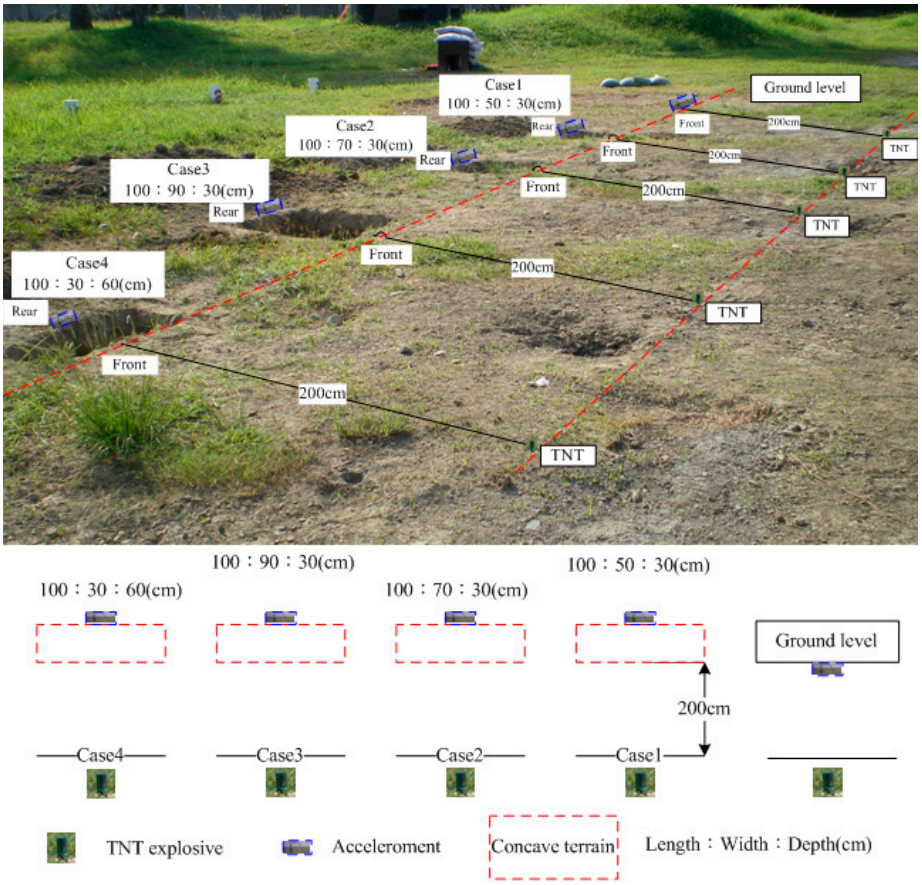

Figure 1. Setup for the concave terrain explosion tests.

2.2. Numerical Analysis

For the numerical simulation analysis, this study employed the finite element (FE) hydrodynamic code LS-DYNA as an analysis tool. In addition, eight-node solid elements and Multi-Material Arbitrary Lagrangian–Eulerian algorithm (MMALE) were applied to a 3D solid structure model, incorporating fluid–solid coupling, to analyze the propagation of blast waves. To verify the reliability of the numerical analysis model, this study examined the impact of topography on the effects of blast vibrations.

Blast analysis involves transient dynamics problems, and, therefore, an effective calculation tool must be used to conduct a transient dynamics analysis. Integration methods in numerical analyses include explicit time integration and implicit time integration. Explicit time integration involves using currently known values to calculate future unknown values, whereas implicit time integration requires an iterative method in order to obtain a solution. Because explicit time integration involves a centered difference scheme, it is ideal for calculating nonlinear problems. For nonlinear FE analysis, LS-DYNA code uses continuum mechanics theories, transient dynamic nonlinear analysis and a centered difference scheme, to conduct explicit time integration calculations.

The explicit time integration method adopted in the LS-DYNA program requires time steps (Δt) smaller than the critical time interval and thus is a conditionally stable calculation method. The program automatically divides the calculation time (T) into $T/\Delta t$ cycle periods. Any element type is stably calculated through control coefficients ranging from 0.1 to 0.9. However, an explosion analysis requires the control parameter (TSSFAC) to be lowered to a default of 0.67. Because blast analysis involves transient dynamics problems, this study employed eight-node hexahedral elements to construct a 3D numerical model for investigating fluid–solid coupling. These elements were defined by eight nodes, generating degrees of freedom of velocity, acceleration and planar movement on the X, Y and Z axes respectively. Because the volume of the model materials cannot equal 0 when subjected to compressive stress or substantial deformation, an explicit dynamics analysis was adopted; the stability functions for the eight-node elements are expressed in Equations (1) and (2); the characteristic length (L_e) is expressed in Equation (3); the wave velocity of elastic materials is expressed in Equation (4); and the wave velocity of elastic materials with a constant bulk modulus is expressed in Equation (5). In addition, this study employed Equation (6), to calculate the minimum time interval for the elements [17].

$$\Delta t_e = \frac{L_e}{\left\{\left[Q + \left(Q^2 + c_v^2\right)^{\frac{1}{2}}\right]\right\}} \tag{1}$$

$$Q = \begin{cases} C_a c_v + C_b L_e \left|\dot{\varepsilon}_{kk}\right| for \dot{\varepsilon}_{kk} < 0 \\ 0 \; for \; \dot{\varepsilon}_{kk} \geq 0 \end{cases} \tag{2}$$

$$L_e = \frac{v_e}{A_{e\max}} \tag{3}$$

$$c_v = \left[\left(\frac{4G}{3\rho_0} + \frac{\partial p}{\partial \rho}\right)_s\right]^{\frac{1}{2}} \tag{4}$$

$$c_v = \sqrt{\frac{E(1-v)}{(1+v)(1-2v)\rho}} \tag{5}$$

$$\Delta t^{n+1} = \alpha \cdot \min\{\Delta t_1, \Delta t_2, \Delta t_3, \cdots, \Delta t_N\} \tag{6}$$

where Δt_e denotes the time steps of solid element; Q denotes the function of volume viscosity coefficients C_a and C_b; L_e refers to the characteristic length; $\dot{\varepsilon}_{kk}$ denotes the strain rate tensor; v_e is the element volume; $A_{e\max}$ refers to the area of the largest side; c_v is the speed of sound in the materials; ρ denotes the mass density; E is Young's modulus; G denotes the shear modulus; v is Poisson's ratio; and N represents the number of elements.

3. Implementation of Numerical Analysis

Adopting the MMALE and eight-node solid elements, this study constructed a 3D numerical model for fluid–solid coupling. Moreover, to examine the effects of topography on the propagation of explosion-induced vibration waves, the Eulerian algorithm was used to define the meshes for the applied explosive and air. The Lagrangian algorithm was used to define the meshes for the soil.

3.1. Numerical Simulation Model

According to the test conditions, this study constructed a numerical analysis model, then conducted an analysis using a 1/2 symmetry model with a non-reflective boundary to simulate a blast in unlimited space [18,19] and set the measurement units as cm, g, μs. The fluid and structure meshes were independent of each other. The density of the structure meshes was twice that of the solid meshes. The fluid–solid coupling was established through an overlapping approach [20]. The coupling definition CONSTRAINED_LAGRANGE_IN_SOLID was used to construct a MMALE fluid–solid coupling

numerical analysis model. Under the ideal gas conditions, the dimensions of the air model were 360 cm × 100 cm × 360 cm (L × W × H). The weight and density of the rectangular TNT explosives (1.64 cm × 1.64 cm × 9.3 cm; L × W × H) were set at 226.796 g (0.5 lb) and 1.63 g/cm^3, respectively. The dimensions of the soil model were 360 cm × 100 cm × 200 cm (L × W × H).

The size of mesh was set according to the minimum width of the TNT explosive [21]. The Eulerian mesh was set as half as high as the minimum length of the explosive. The time-step control coefficient was set at 0.3 [21]. The FE mesh of the soil was set at 1.64 cm × 1.64 cm × 3.28 cm (L × W × H). Figure 2 shows a 1/2 symmetry model for the concave terrain and convex terrain numerical analysis. The length of the concave terrain was set at 100 cm. The width (W) and depth (D) of Cases 1–4 were set at 50 cm × 30 cm, 70 cm × 30 cm, 90 cm × 30 cm, and 30 cm × 60 cm, respectively. The length of the convex terrain was set at 100cm. The width (W) and height (H) of Cases 5–10 were set at 50 cm × 30 cm, 70 cm × 30 cm, 90 cm × 30 cm, 30 cm × 30 cm, 30 cm × 60 cm, and 30 cm × 90 cm, respectively. Furthermore, a simulation analysis was conducted on the changes in the attenuation and amplification effects of blast waves over time and space.

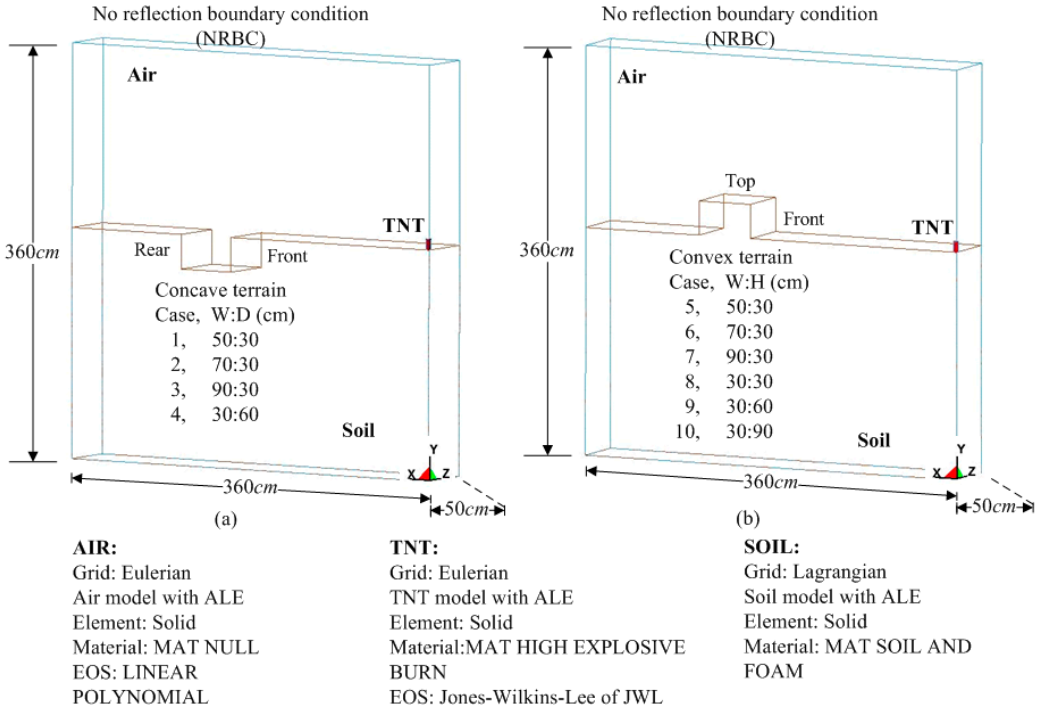

Figure 2. 1/2 symmetry model for the numerical analysis. (**a**) 1/2 symmetry model for the concave terrain numerical analysis; (**b**) 1/2 symmetry model for the convex terrain numerical analysis.

3.2. Mathematical Formulation of Material Parameters and Equation of State

Table 1 lists the material parameters of the air and TNT. The constitutive law of materials must be paired with corresponding equations of state (EOS) to analyze the relationship among material volume, stress, and strain. Various EOSs were used to describe the changes in the material's pressure, internal energy, density, and volume, from the explosions. This study adopted the MAT_NULL material mode in the air model, and used EOS_LINEAR_POLYNOMIAL as an EOS, to describe the characteristics of the Equation (7) [17]. The material parameters adopted were pressure (p), mass density (RO), volume (V) determined by relative volume (V/V_0) for erosion in tension (TEROD) and relative volume (V/V_0) for erosion in compression (CEROD), Young's modulus (YM), Poisson's ratio (PR), constants $C_0 = C_1 = C_2 = C_3 = C_6 = 0$ and $C_4 = C_5 = \gamma - 1$ with γ representing the rate of change to the

specific air temperature, initial of the relative volume (V_0), initial energy of the unit volume (E_0), pressure cutoff (PC), and dynamic viscosity coefficient (MU; $\mu = 1/V - 1$).

$$P = C_0 + C_1 + C_2\mu^2 + C_3\mu^3 + \left(C_4 + C_5\mu + C_6\mu^2\right)E_0 \tag{7}$$

Table 1. Material parameters of air and TNT explosive.

Element	Material and Equation of State Parameters (Unit System: g, cm, μ-Second)						
Air	MAT_NULL						
	RO	PC	MU	TEROD	CEROD	YM	PR
	0.00129	0.0	0.0	0.0	0.0	0.0	0.0
	EOS_LINEAR_POLYNOMIAL						
	C_0	C_1, C_2, C_3, C_6		C_4	C_5	V_0	E_0
	-1.07×10^{-6}	0.0		0.4	0.4	1.0	2.53×10^{-6}
TNT	MAT_HIGH_EXPLOSIVE_BURN						
	RO	D	PCJ	BETA	K	G	SIGY
	1.63	0.693	0.21	0.0	0.0	0.0	0.0
	EOS_JWL						
	A	B	R_1	R_2	OMEGA (ω)	E_0	V_0
	3.712	0.03231	4.15	0.95	0.3	0.07	1.0

The Jones–Wilkins–Lee (JWL) equation of state is an analytical EOS used in the modeling of high explosives. This study applied the MAT_HIGH_EXPLOSIVE_BURN material mode in the explosive model and used EOS_JWL as the EOS for simulating a high-intensity explosion, by using Equation (8). The EOS parameters were the relative volume, initial energy of the unit volume (E_0), material internal energy (E_m), and constants for the explosive characteristics A, B, R_1, R_2, and OMEGA (ω) [18]. By referring to an explosives manual released by Lawrence Livermore National Laboratory [22], this study adopted the following material parameters for the TNT: mass density (RO), bulk modulus (K), shear modulus (G), yield stress (SIGY), blast velocity (D), Chapman–Jouguet pressure (PCJ), and beta burn flag (BETA).

$$P = A\left(1 - \frac{\omega}{R_1 V}\right)E_m^{-R_1 V} + B\left(1 - \frac{\omega}{R_2 V}\right)E_m^{-R_2 V} + \frac{\omega E_0}{V} \tag{8}$$

Table 2 presents the material parameters of soil, a compressible, porous material. The yield criterion adopted by Krieg was developed based on plasticity theory. Post-yield behaviors of materials include hydrostatic pressure and shear stress. This soil model facilitates analyzing material failure under stress. The yield function (f) adopted in this study was derived from Equation (9). LS-DYNA was used to observe the relationship between the average stress and failure intensity in the shear stress failure of materials under stress. This study employed the MAT_SOIL_AND_FOAM material mode to analyze the propagation of blast waves in soil [17,18]. The applied soil parameters included mass density (RO), shear modulus (G), bulk modulus (K), and pressure cutoff (C). The water content of the soil used for the indoor tests was 10.27% ($c = 0.95 kg/cm^2$; $\phi = 36°$). According to the Unified Soil Classification System, the soil was sand, with characteristics of clay (classified as SC).

$$f = [J_2 - (a_0 + a_1 p + a_2 p^2)], \tag{9}$$

with $a_0 = c^2$, $a_1 = 2c\tan\phi$, $a_2 = \tan^2\phi$, where J_2 is the second invariant of deviatoric stress; p is the pressure; and $a_0 a_1 a_2$ are the shear force yield surface parameters.

Table 2. Material parameters of air and TNT explosive.

Soil	MAT_SOIL_AND_FOAM					
	RO	G	BULK	A_0	A_1	A_2
	2.6	0.000147	0.00729	9.025×10^{-12}	1.380×10^{-11}	5.280×10^{-12}

4. Results and Discussion

4.1. In Situ Explosion Tests

Figures 3 and 4 illustrate the ground acceleration curves for the front and rear of the concave terrain, respectively. The results of the explosion tests, conducted with the same amount of TNT, indicated that, when the depth of the concave terrain was set at 30 cm, the ground acceleration was attenuated with increasing terrain width. The results showed that the concave terrain had substantial attenuation effects on the propagation of blast waves. Thus, the attenuation effects were associated with the width and depth of the concave terrain; moreover, the terrain depth had a more substantial effect than the terrain width.

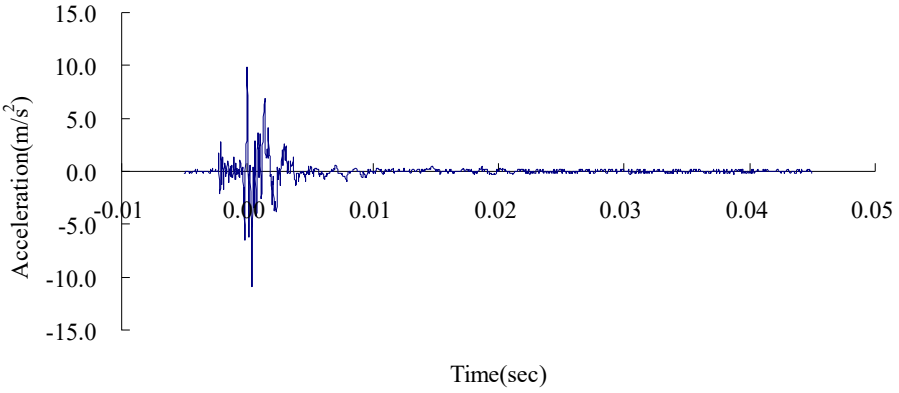

Figure 3. Vertical ground acceleration curve for the front of the concave terrain.

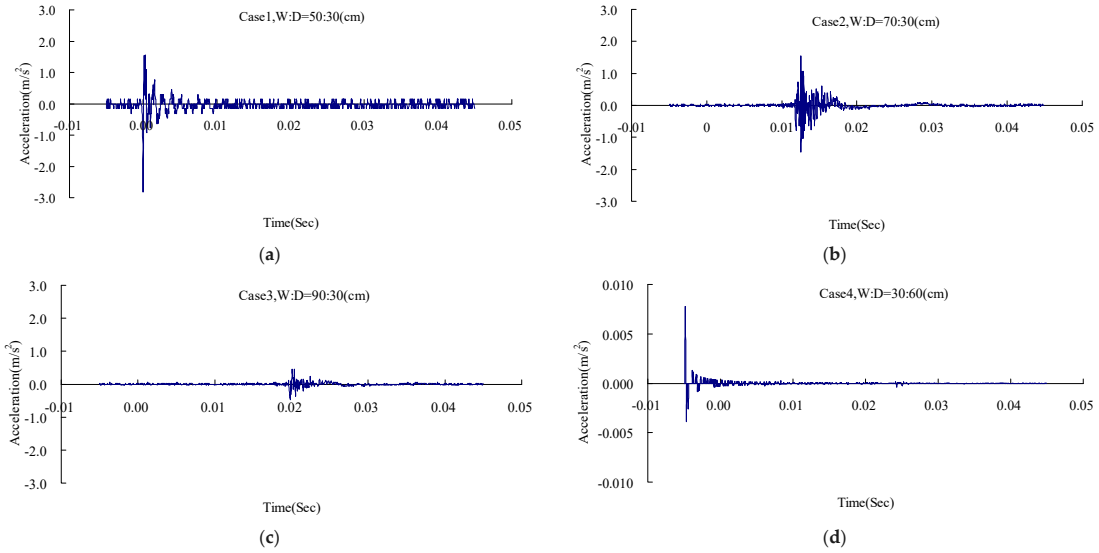

Figure 4. Vertical ground acceleration curve for the rear of the concave terrain. (**a**) Case1, width:depth = 50:30 cm; (**b**) Case2, width:depth = 70:30 cm; (**c**) Case3, width:depth = 90:30 cm; (**c**) Case3, width:depth = 90:30 cm.

4.2. Comparison Simulation Results by the Explosion Tests

The vertical PGA values observed in the previous tests were employed to verify the numerical analysis results, which were then used to investigate the impact of the concave terrain on the propagation of blast wave energy. An error analysis was conducted on the numerical analysis results and the PGA values collected from the explosion tests (relative error percentage (%)) = (PGA from numerical analysis—PGA from explosion tests)/PGA from explosion tests × 100%. Table 3 lists the PGA and relative error values derived from the explosion tests and numerical analysis. Figures 5 and 6, respectively, demonstrate the vertical ground acceleration curves for the front and rear of the concave terrain cases. The overall relative error between the test and numerical analysis results fell within 15%, thereby confirming the results of previous studies [5] and verifying the accuracy of the applied numerical analysis model. In addition, the study results showed that the propagation and variation processes of blast waves can be effectively analyzed by employing eight-node solid elements and a MMALE algorithm for developing a numerical analysis model examining fluid–solid coupling.

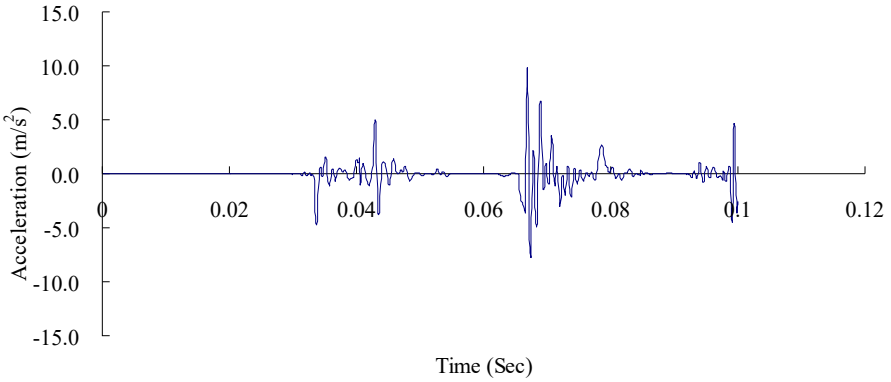

Figure 5. Vertical ground acceleration curve for the front of the concave terrain (numerical analysis).

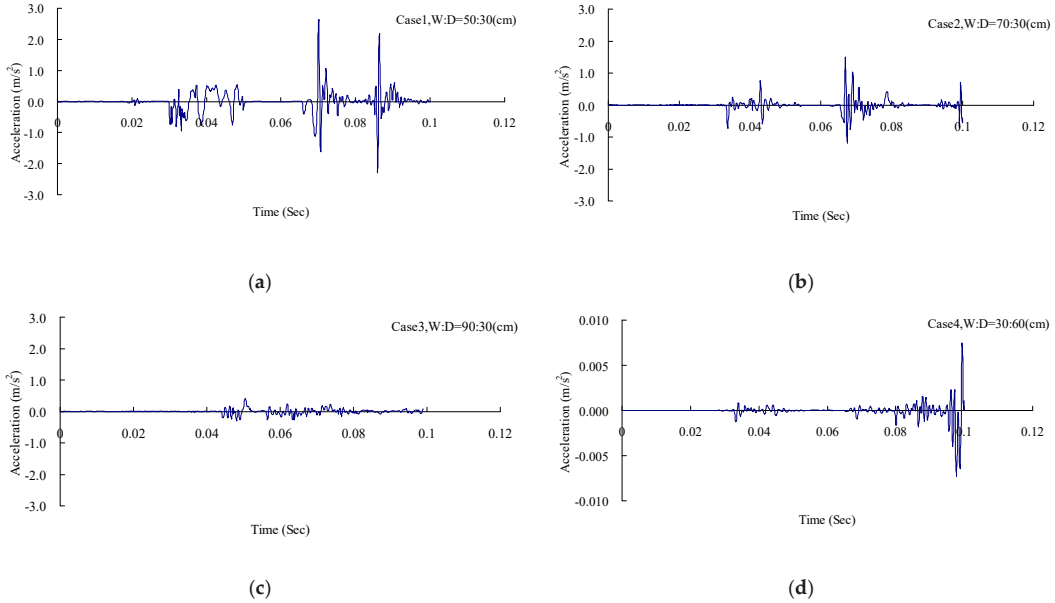

Figure 6. Vertical ground acceleration curve for the rear of the concave terrain (numerical analysis). (**a**) Case1, width:depth = 50:30 cm; (**b**) Case2, width:depth = 70:30 cm; (**c**) Case3, width:depth = 90:30 cm; (**d**) Case4, width:depth = 30:60 cm.

Table 3. Vertical PGA and relative errors from the explosion tests and numerical analysis.

Case	W:D (cm)	Experiment (m/s^2)	Numerical Analysis (m/s^2)	Relative Error (%)
Front of concave		10.0500	9.7326	−3.158
Rear of concave				
1	50:30	2.7690	2.6309	−4.987
2	70:30	1.5500	1.4946	−3.574
3	90:30	0.4500	0.4135	−8.107
4	30:60	0.0078	0.0074	−4.600

4.3. Topographical Effects of the Propagation of Blast Waves

Table 4 lists the horizontal PGA of the concave terrain from numerical analysis. Analysis of the effects of the width and depth of the concave terrain revealed that, when the explosion energy and terrain depth were fixed, and the terrain width was increased proportionately, the ground acceleration was attenuated. However, peak attenuation was observed when the width of the terrain was reduced proportionately, and the depth was doubled. The results of the tests and numerical analysis indicated that the concave terrain had considerable attenuation effects on the propagation of blast waves. The attenuation effects were associated with the width and depth of the concave terrain. Moreover, the terrain depth led to more substantial attenuation effects than the terrain width, and the horizontal attenuation effects were more pronounced than the vertical ones.

Table 4. Horizontal PGA of the concave terrain from the numerical analysis.

Case	W:D (cm)	Front of Concave (m/s^2)	Rear of Concave (m/s^2)
1	50:30	9.6817	2.4275
2	70:30		1.1833
3	90:30		0.4071
4	30:60		0.0061

Table 5 lists the vertical and horizontal PGA of the convex terrain from numerical analysis. By using Cases 5–7 to analyze the effects of the terrain width, this study set the terrain height at 30 cm and increased the width to 50, 70 and 90 cm, in a constant increment of 20 cm. A comparison of the ground acceleration of the convex terrain showed that the convex terrain had an inhibiting effect on the blast energy. Cases 8–10 were used to analyze the effects of the terrain height, by setting the terrain width at 30 cm and configuring the height as 30, 60 and 90 cm.

Table 5. Vertical and horizontal PGA of the convex terrain from the numerical analysis.

Case	W:H (cm)	Vertical PGA (m/s^2)		Horizontal PGA (m/s^2)	
		Front of Convex	Central of Top	Front of Convex	Central of Top
5	50:30	8.9179	40.0893	7.6326	19.5180
6	70:30		29.2753		14.4296
7	90:30		22.7200		10.8512
8	30:30		41.5224		20.2410
9	30:60		43.5458		21.7863
10	30:90		37.9214		18.1338

The analysis results indicated that the ground acceleration of the top of the convex terrain was higher than at the ground surface, and gradually increased with the terrain height. Therefore, the propagation of blast waves in the convex terrain exhibited both attenuation and amplification effects. In the convex terrain, the amplification effects of vertical blast waves were larger than those of horizontal ones, indicating that the directionality of wave propagation affects the attenuation and amplification of blast waves. In addition, higher elevation differences led to more noticeable amplification effects. At a fixed height, the amplification effects increased as width decreased.

5. Conclusions

Controlling explosion hazards is a crucial aspect of safety protection. Explosion intensity exceeding normal levels affects the safety of people and facilities, and, thus, requires vibration reduction for hazard mitigation. To analyze the effects of topography on ground explosions, this study adopted the concept of explosion control to examine the effects of topography on the propagation of blast waves. In addition, this study applied vibration control to disaster risk reduction. The findings may serve as a reference for blast hazard control and disaster prevention. The results of this study are listed below:

1. This study measured ground acceleration values during in situ explosion tests to verify the relative error by numerical analysis. The analysis results indicate that incorporating MMALE with eight-node solid elements, and constructing a numerical analysis model for explosions, is effective for analyzing fluid–solid coupling effects, solving dynamics problems (e.g., geometric nonlinearity, material nonlinearity, and contact nonlinearity), and facilitating an examination of the variations in blast wave energy, to provide a foundation for developing explosion hazard analysis models.
2. Blast analysis involves transient dynamics problems. It is generally used for analyzing blasts with rapid loading times and high vibration frequencies, and involves highly nonlinear geometries and materials. The propagation of blast waves in a medium is affected by the properties of that medium. Concave terrain has considerable attenuation effects on the propagation of blast waves. The attenuation is associated with the width and depth of concave terrain, although the depth has a more pronounced effect. The horizontal attenuation effects from horizontal waves are more prominent than those from vertical waves, and the effects are subject to the direction in which the wave propagates. The propagation of blast waves in convex terrain exhibits both attenuation and amplification effects. In convex terrain, vertical blast waves have stronger amplification effects than horizontal ones, indicating that larger elevation differences lead to more noticeable amplification effects. The amplification effects decrease as the width of convex terrain increases. The study results may serve as a reference for vibration isolation engineering and disaster prevention construction.
3. Seismic waves induced by explosions are a process of energy propagation and transfer. Therefore, to achieve the goals of vibration reduction, disaster prevention, and safety protection, designers of blast protection engineering projects can measure the energy of explosions that induce ground vibrations, to obtain a reference for vibration hazard control, secure structures with substantial elevation differences, and minimize blast wave hazards by digging vibration reduction trenches.

Funding: This research was supported by the Ministry of Science and Technology, Taiwan, R.O.C., project number: MOST 104-2221-E-145-004, MOST 107-2221-E-145-001.

Conflicts of Interest: The authors declare no conflict of interest.

References

1. Crandle, F.J. Ground vibration due to blasting and its effect upon structures. *J. Boston Soc. Civ. Eng.* **1949**, *36*, 222–245.
2. Wang, J. *Simulation of Landmine Explosion Using LS-DYNA 3D Software: Benchmark Work of Simulation in Soil and Air*; DSTO-TR-1168; Aeronautical and Maritime Research Laboratory: Fishermans Bend, VIC, Australia, 2001; pp. 1–30.
3. Wang, T.C.; Lee, C.Y.; Wang, I.T. Analysis of blasting vibration wave propagation based on finite element numerical calculation and experimental investigations. *J. Vibroeng.* **2017**, *19*, 2703–2712. [CrossRef]
4. Goodman, H.J. *Compiled Free-Air Blast Data on Bare Spherical Pentolite*; BRL Report, No. 1092; Ballistic Research Laboratories: Aberdeen, MD, USA, 1960; pp. 3–46.
5. Kivity, Y.; Ben-Dor, G.; Anteby, I.; Sadot, O. The blast wave resulting from an accidental explosion in an ammunition magazine. In Proceedings of the Military Aspects of Blast and Shock Symposium–19th International Conference, Calgary, AB, Canada, 2–6 October 2006.

6. Koga, Y.; Matsuo, O. Shaking table tests of embankments resting on liquefiable sandy ground. *Soil. Found.* **1990**, *30*, 162–174. [CrossRef]
7. Wang, Z.Q.; Lu, Y. Numerical analysis on dynamic deformation mechanism of soils under blast loading. *Soil. Dyn. Earthq. Eng.* **2003**, *23*, 705–714. [CrossRef]
8. Khandelwal, M.; Singh, T.N. Evaluation of blast-induced ground vibration predictors. *Soil. Dyn. Earthq. Eng.* **2007**, *27*, 116–125. [CrossRef]
9. Ak, H.; Iphar, M.; Yavuz, M.; Konuk, A. Evaluation of ground vibration effect of blasting operations in a magnesite mine. *Soil. Dyn. Earthq. Eng.* **2009**, *29*, 669–676. [CrossRef]
10. US Army Engineers Waterways Experimental Station. *Fundamental of Protection Design for Conventional Weapons*; Technical Manual TM 5-855-1; US Army Engineers Waterways Experimental Station: Washington, DC, USA, 1998.
11. Ahmad, S.; Al-Hussaini, T.M. Simplified design for vibration screening by open and in-filled trenches. *J. Geotech. Eng.* **1991**, *117*, 67–88. [CrossRef]
12. Klein, R.; Antes, H.; Le Houedec, D. Efficient 3D Modelling of Vibration Isolation by Open Trenches. *Comput. Struct.* **1997**, *64*, 809–817. [CrossRef]
13. Spyros, S.; Fotis, R. Computer simulation of shock waves transmission in obstructed. *J. Los. Pre. Pro. Ind.* **2004**, *17*, 407–417.
14. Dally, J.W.; David, L. A photoelastic analysis of propagation of Rayleigh waves past a step change in elevation. *Bull. Seism. Soc. Am.* **1968**, *58*, 539–563.
15. Zhu, Z.; Yang, Y. Research on effect decreasing quake of groove on the building with dynamic photo elasticity. *Exp. Shock Wav.* **1989**, *9*, 55–60.
16. Zhang, Q.; Bia, C.H.; Liu, Q.M. Experimental research on amplitude change of blasting seismic wave with topography. *J. Be. Inst. Tech.* **2000**, *9*, 237–242.
17. *LS-DYNA Theoretical Manual*; Livermore Software Technology Corporation: Livermore, CA, USA, 2006.
18. *LS-DYNA Keyword User's Manual*; Livermore Software Technology Corporation: Livermore, CA, USA, 2009.
19. Tai, Y.S.; Chu, T.L.; Hu, H.T.; Wu, J.Y. Dynamic response of a reinforced concrete slab subjected to air blast load. *Theo. Appl. Fract. Mech.* **2011**, *56*, 140–147. [CrossRef]
20. Gebbeken, N.; Ruppert, M. On the safety and reliability of high dynamic hydrocode simulations. *Int. J. Num. Meth. Eng.* **1999**, *46*, 839–851. [CrossRef]
21. Wang, I.T. Numerical and experimental verification of finite element mesh convergence under explosion loading. *J. Vibroeng.* **2014**, *16*, 1786–1798.
22. Dobratz, B.M. *LLNL Explosive Handbook Properties of Chemical Explosives and Explosive Simulants*; Lawrence Livemore National Laboratory: Livermore, CA, USA, 1981.